



HAL
open science

SPAD array sensitivity enhancement by diffractive microlens

Jérôme Vaillant, Lilian Masarotto, Romain Paquet, Véronique Lecoutre,
Catherine Pellé, Norbert Moussy, Sébastien Jouan

► **To cite this version:**

Jérôme Vaillant, Lilian Masarotto, Romain Paquet, Véronique Lecoutre, Catherine Pellé, et al.. SPAD array sensitivity enhancement by diffractive microlens. IISW 2017 - 2017 International Image Sensor Workshop, International Image Sensor Society, May 2017, Hiroshima, Japan. hal-04235027

HAL Id: hal-04235027

<https://hal.science/hal-04235027>

Submitted on 10 Oct 2023

HAL is a multi-disciplinary open access archive for the deposit and dissemination of scientific research documents, whether they are published or not. The documents may come from teaching and research institutions in France or abroad, or from public or private research centers.

L'archive ouverte pluridisciplinaire **HAL**, est destinée au dépôt et à la diffusion de documents scientifiques de niveau recherche, publiés ou non, émanant des établissements d'enseignement et de recherche français ou étrangers, des laboratoires publics ou privés.

SPAD array sensitivity enhancement by diffractive microlens

J. Vaillant*, L. Masarotto*, R. Paquet*, V. Lecoutre*, C. Pellé*, N. Moussy* and S. Jouan†

*Univ. Grenoble Alpes, CEA, LETI, DOPT, LIS, F-38000 Grenoble

†TR&D, STMicroelectronics, 850 rue Jean Monnet, F-38920 Crolles

Abstract—In this paper we present sensitivity improvement of SPAD pixel using diffractive microlens. We designed microlens structures based on rigorous optical simulations, then we developed the process for thick optical spacer and thin amorphous silicon deposition, on which diffractive structures were defined by lithography and etching. These microlenses have been implemented two SPAD designs available on STMicroelectronics 40nm CMOS testchips (32×32 SPAD array). Circuits were characterized and we demonstrated, depending on SPAD design, high optical gain at $850nm$ ($\times 3$ to $\times 8$) and significant gain at $940nm$ ($\times 2$ to $\times 2.5$).

I. INTRODUCTION

Single Photon Avalanche Diode (SPAD) arrays are promising image sensors for applications requiring photon arrival timestamp with accuracy around hundreds of picoseconds or even less. From an optical point of view, the main limitation of SPAD pixels is their low optical fill-factor (ff_o), about 10% or below. This can be partially overcome by placing light concentrator in front of each pixel. External microlenses, either refractive or diffractive, have first been implemented [1] with limitation of alignment accuracy between microlens and SPAD arrays. More recently on-chip refractive microlens arrays, fabricated at wafer level with conventional reflow process, were demonstrated with success[2].

In this work, we present the development of wafer level diffractive microlens on top of SPAD for applications in near-infrared (between 850nm and 950nm). In the following, we detail the SPAD designs and the optical simulations performed to optimize the diffractive structures. Then, the specific process we developed is presented before summarizing electro-optical characterization results obtained on test-chips.

II. SPAD DESIGNS

In our work we considered two SPAD layouts, both on Front-Side Illumination (FSI) STMicroelectronics 40nm CMOS technology[3]. For each design, the pixel has a pitch of $21.6\mu m$ and is implemented in a 32×32 array. The first one has a conventional layout: diode with rounded square shape and metal shielding (see Fig. 1a).

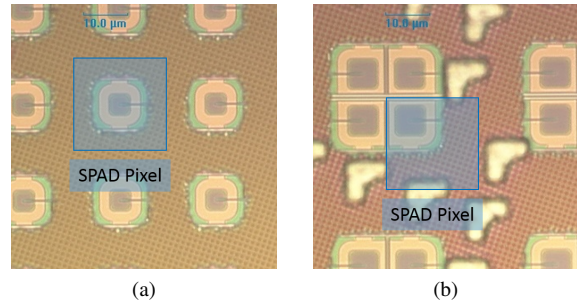


Fig. 1. Layout of SPAD pixels: (a) periodic design with fill-factor of 5%, (b) grouped design with fill-factor of 12%.

The optical fill-factor $ff_o = 5\%$ is defined by the size of the metal window $4.7 \times 4.7\mu m^2$. In the second design, the N-well of diodes are shared between 2×2 SPAD, improving the fill-factor $ff_o = 12\%$ with a size of metal window of $7.5 \times 7.5\mu m^2$, see Fig. 1b.

III. OPTICAL SIMULATIONS

To concentrate light onto SPAD photodiode, we considered Fresnel Zone Plate[4, 5] structures (FZP). It consists of rings diffracting the light to produce constructive interference at the focal point and size of rings are calculated using Fresnel zone concept[6, 7]. In order to take profit of all incident light, a $k\lambda/2$ (with $k \in \mathbb{N}^*$) phase shift must be introduced by the material of the rings, so light diffracted in-between rings and by rings adds constructively at the lens focus.

We chose amorphous silicon (a:Si) for the rings as it presents advantageous properties: it is compatible with CMOS process, has very low absorption in the spectrum of interest and thanks to its high refractive index (see Fig. 2), the $k\lambda/2$ phase shift can be introduced while keeping the layer thickness low, further reducing the absorption and making the patterning easier. As the pitch of the SPAD is quite large ($21.6\mu m$) compared to the back-end of line (BEOL) thickness ($6.1\mu m$), we introduced an optical spacer between the FZP and the wafer. This pedestal has to be transparent and with a

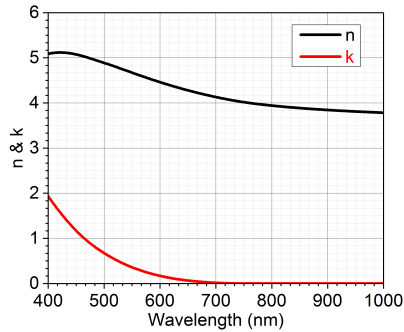


Fig. 2. Refractive and extinction indices of amorphous silicon.

low refractive index, thus silicon oxide is an appropriate material.

The objective of the optical simulations is to identify the parameters that define the FZP structures to be implemented on mask. Few parameters are required: the thickness of the optical spacer, the thickness of the a:Si layer and the effective focal length of the FZP, considering light propagates in silicon oxide before reaching the silicon. Thus, we performed 3D rigorous electro-magnetic simulations[8] with FDTD-Solutions software[9] which include the model of the SPAD, based on its layout and CMOS 40nm technology description (see Fig. 3). The model is illuminated by plane waves

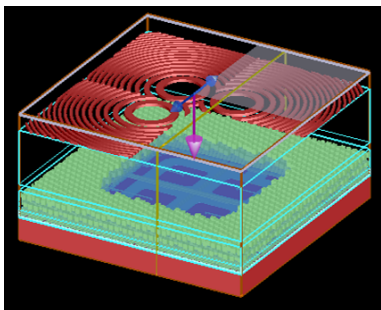


Fig. 3. 3D model of 2×2 SPAD pixel (see Fig. 1b): silicon in red at the bottom, metal lines in blue and green and FZP structures in red on the top of the model.

and the electric field inside the structure is recorded as shown in Fig. 4. Our figure of merit is amount of light absorbed in a volume defined by the photodiode N-well. In order to limit the process trials, after a first optimization, we fixed the thickness of the silicon oxide pedestal to $10\mu m$. Then we finely optimized the two remaining parameters (a:Si layer thickness and FZP focal length). Nevertheless, as the simulation time is very long for such pixels, we strongly limited the number of simulation runs by using metamodelization frame-

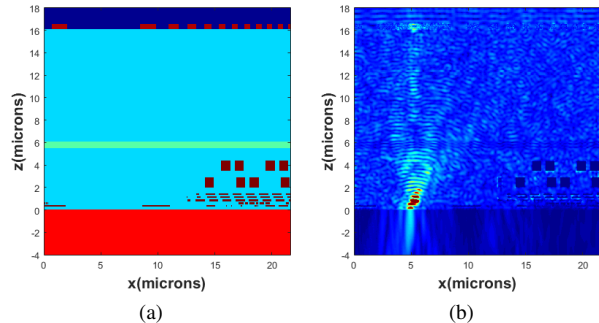


Fig. 4. Vertical cross-sections of model presented in Fig. 3: (a) refractive index of the structure and (b) simulated electrical field.

work or Surrogate Based Design Optimization (SBDO) developed at CEA-LETI[10]. With only few tens of simulations, the optimum was found. For instance, for the 2×2 SPAD, results are shown in Fig. 5. In this case, optimum is reached for $f_{effective} = 15.5\mu m$ and a a:Si thickness of $465nm$, introducing a $3/2\lambda$ phase shift when light passes through the rings.

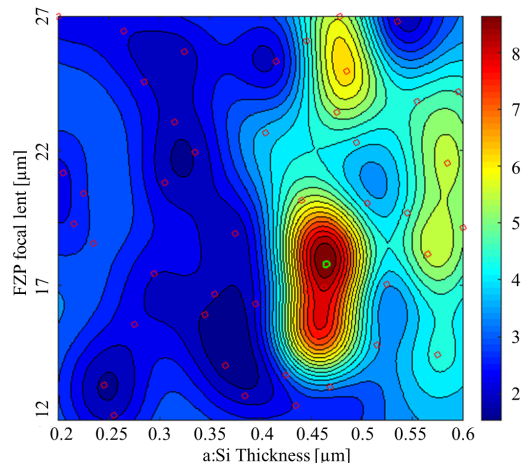


Fig. 5. Results of SBDO for 2×2 SPAD pixel as a function of a:Si thickness and FZP effective focal length. The point highlighted in green is the estimated optimum.

In addition to this simulated optimal design, we tested several FZP designs by increasing the effective focal length and using as nominal wavelength the standard laser diode emission wavelength ($850nm$, $905nm$ and $940nm$) (see tables I and II for all combinations).

IV. PROCESS DEVELOPMENT

The two main components required for the realization of the diffractive structures are the optical spacer and the amorphous silicon structures. The first one is made by thick oxide deposition and need to fulfill several constrains: a thickness of $10\mu m$, a low refractive index

(around 1.5), a low temperature deposition for back-end compatibility (below $400^{\circ}C$) and low mechanical stress to ensure a minimum bow on the wafer for the lithography done afterward (maximum allowed sag over the wafer is $100\mu m$). Thus, we developed a SiO_2 PECVD deposition at $350^{\circ}C$, giving us a layer with a refractive index of $1.52@633nm$ and a maximum sag on $300mm$ wafer below $10\mu m$.

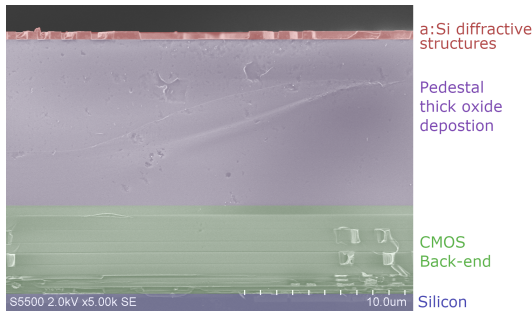


Fig. 6. Vertical cross-section of optical spacer and a:Si microlens processed on CMOS wafer

The a:Si layer shares the same constraints in terms of process compatibility: a low temperature deposition and a low mechanical stress. In addition we took a special attention to the absorption coefficient in the spectral range of interest (above $800nm$). By tuning the RF power, precursor flux and pressure of our PECVD tool, we were able to deposit a a:Si layer with a thickness of $465nm$ while keeping the sag on the wafer below $80\mu m$, compatible with the lithography scanner.

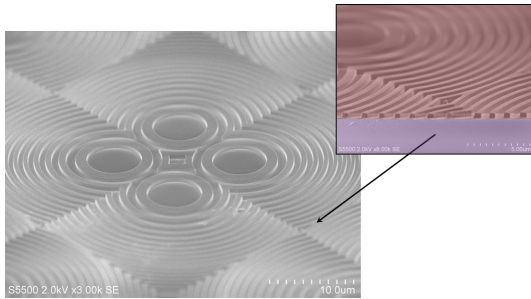


Fig. 7. Tilted SEM view of FZP structures implemented on 2×2 SPAD.

Finally we worked on the lithography and the etching of the a:Si layer. The exposure and focus were tune to ensure the capability to define pattern with a critical dimension of $CD = 100nm$ and a space of $100nm$ (see Fig. 7).

In order to implement few design variants of FZP on the 32×32 SPAD arrays while ensuring statistically representative sampling, we split the image into 8 areas of 8×16 SPADs. One of them was kept free from

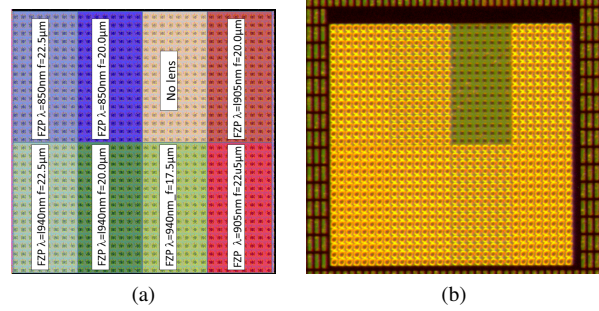


Fig. 8. Implementation of diffractive microlens on 32×32 circuit, (a) view of layout, (b) optical microscope.

microlens and serves as reference for measurement, avoiding intra and inter wafer variations (see Fig. 8).

V. ELECTRO-OPTICAL CHARACTERIZATION RESULTS

On processed wafers, devices were characterized using in-house characterization capability. Thus, spectral response, or photon detection efficiency, was measured with spectrally and spacially controlled diffuse light ($\Delta\lambda = 10nm$ and $f_{\#} = 2$). For each die, mean value and standard deviation over the 8×16 SPADs area are computed and one example is reported on Fig. 9.

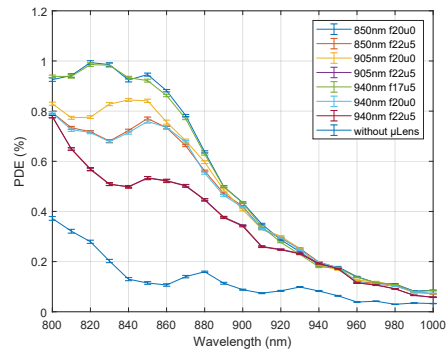


Fig. 9. Spectral photon detection efficiency for bare SPAD and for eight diffractive microlens variants, for centered SPAD design. **to be updated**

Based on these PDE curves, we computed the optical gain provided by diffractive microlens at three wavelength ($850nm$, $905nm$ and $940nm$) corresponding to standard laser diodes. This gain is computed for several dice over the wafer and mean value and standard deviation is reported on table I and table II. We achieved an optical gain of $\times 8$ at $850nm$ for centered SPAD design, and $\times 3$ at $850nm$ for off-centered SPAD design. This latter lower gain is at first due to the $2.4\times$ higher optical fill factor ($ff_o = 12\%$ versus $ff_o = 5\%$) and the strong off-axis that make the light concentration more difficult.

TABLE I
OPTICAL GAIN OF DIFFRACTIVE MICROLENS ON CENTERED SPAD. **TO BE UPDATED**

FZP design		optical gain		
λ_{design}	$f_{effective}$	@850nm	@905nm	@940nm
850nm	20.0 μ m	4 \pm 0.2	3.5 \pm 0.3	2 \pm 0.5
850nm	22.0 μ m	4 \pm 0.2	3.5 \pm 0.3	2 \pm 0.5
905nm	20.0 μ m	4 \pm 0.2	3.5 \pm 0.3	2 \pm 0.5
905nm	22.0 μ m	4 \pm 0.2	3.5 \pm 0.3	2 \pm 0.5
940nm	17.5 μ m	4 \pm 0.2	3.5 \pm 0.3	2 \pm 0.5
940nm	20.0 μ m	4 \pm 0.2	3.5 \pm 0.3	2 \pm 0.5
940nm	22.5 μ m	4 \pm 0.2	3.5 \pm 0.3	2 \pm 0.5

TABLE II
OPTICAL GAIN OF DIFFRACTIVE MICROLENS ON 2 \times 2 SPAD. **TO BE UPDATED**

FZP design		optical gain		
λ_{design}	$f_{effective}$	@850nm	@905nm	@940nm
940nm	15.5 μ m	4 \pm 0.2	3.5 \pm 0.3	2 \pm 0.5
940nm	17.5 μ m	4 \pm 0.2	3.5 \pm 0.3	2 \pm 0.5
940nm	20.0 μ m	4 \pm 0.2	3.5 \pm 0.3	2 \pm 0.5

VI. CONCLUSION

In this study, we have successfully demonstrated the capability to improve SPAD sensitivity by using diffractive microlenses in the near infrared. Relying on Fresnel Zone Plate structures, we designed the microlenses based on optical simulations taking into consideration the SPAD layout and CMOS technology. Specific process was developed for the optical spacer, made on thick oxide deposition, and the microlenses, made by patterning of amorphous silicon layer. These microlenses were implemented on STMicroelectronics 40nm CMOS testchips and we measured a sensitivity improvement up to a factor 8 \times at 850nm for SPAD having a pitch of 21.6 μ m and bare fill-factor of 5%. To the best of our knowledge these are the highest optical gain demonstrated with diffractive microlens on SPAD, comparable or exceeding results obtain with refractive microlens. This technology offers several advantages like planar and inorganic microlens or the capability to design off-axis microlens.

REFERENCES

- [1] G. Intermite et al. "Enhancing the Fill-Factor of CMOS SPAD Arrays Using Microlens Integration". In: *Proceedings of SPIE*. Vol. 9504. SPIE, 2015. DOI: 10.1117/12.2178950.
- [2] A. R. Ximenes et al. "A 256x256 45/65nm 3D-Stacked SPAD-Based Direct TOF Image Sensor for LiDAR Applications with Optical Polar Modulation for up to 18.6dB Interference Suppression". In: *2018 IEEE International Solid - State Circuits Conference - (ISSCC)*. Feb. 2018, pp. 96–98. DOI: 10.1109/ISSCC.2018.8310201.
- [3] S. Pellegrini et al. "Industrialised SPAD in 40 Nm Technology". In: *2017 IEEE International Electron Devices Meeting (IEDM)*. Dec. 2017, pp. 16.5.1–16.5.4. DOI: 10.1109/IEDM.2017.8268404.
- [4] V. Rochus et al. "Pixel Performance Enhancement by Integrated Diffractive Optics". In: *International Image Sensor Workshop*. 2015.
- [5] Sheng-Chuan Cheng et al. "Lens Solution for Intensity Enhancement in Large-Pixel Single-Photon Avalanche Diode". In: *International Image Sensor Workshop*. Hiroshima, 2017.
- [6] Max Born et al. *Principles of Optics: Electromagnetic Theory of Propagation, Interference and Diffraction of Light*. 7th ed. Cambridge University Press, 1999. ISBN: 978-0521642224. DOI: 10.1017/CBO9781139644181.
- [7] Daniel G. Smith. "Fresnel Zone Plate". In: *Field Guide Phys. Opt.* (Apr. 2013), pp. 49–50. DOI: 10.1117/3.883971.ch48.
- [8] A. Crocherie et al. "Three-Dimensional Broadband FDTD Optical Simulations of CMOS Image Sensor". In: vol. 7100. 2008, 71002J-71002J-12. DOI: 10.1117/12.797417.
- [9] *High-Performance Nanophotonic Simulation Software*. <https://www.lumerical.com/>.
- [10] *Surrogate Based Design Optimization Toolbox*. <https://github.com/freeSBDO/SBDOT>.